

# The Significance of the Production Process of FRP Parts for the Performance in Crashworthiness

Christian Liebold, Andrea Erhart, André Haufe

*DYNAMore GmbH, Industriestr. 2, 70565 Stuttgart, Germany*

## Abstract

*As there is a trend in the automotive industry towards using FRP composites for reducing the weight of vehicles, adequate simulation tools to effectively and accurately predict the structural response of composite structures in crashworthiness are needed.*

*Due to the manufacturing induced fiber orientation, which is particularly for short fiber reinforced composites locally varying, the pointwise mechanical behavior of (S)FRP is a priori unknown and accordingly the prediction of the mechanical behavior of FRP-components is challenging. A promising approach is an analysis that covers the complete process chain from the molding process to the crashworthiness modelling: fiber orientation are determined by process simulation and transferred to the structural analysis model through a data-mapper. Using this information, the local anisotropic material behavior can be determined by means of a homogenization procedure and used for the structural analysis.*

*In this paper two recently implemented possibilities for LS-DYNA<sup>®</sup> are presented. For the first approach, the data-mapper "DYNAmap" transfers the fiber orientation tensor, which is evaluated in a MoldFlow<sup>®</sup> simulation, to the structural analysis model. Using a recently developed constitutive model, pointwise effective anisotropic material properties for this composite are automatically determined and used for the structural simulation. This calculation of homogenized macroscopic properties is done in two steps: At first, effective properties of an associated "pseudo uni-directional" composite are determined by analytical homogenization (see Dvorak [2013]). In a second step an orientation averaging of these uni-directional properties in accordance with the mapped local fiber orientation is carried out; see Advani & Tucker [1987]. While for elasticity the determination of effective properties is done only once in a preprocessing step, for considering inelastic behavior, an update of the material properties during the simulation is necessary from time to time.*

*Alternatively, DYNAmap provides the possibility to perform a homogenization for evaluating the pointwise effective anisotropic elastic stiffness parameters and to transfer the resulting local stiffness values to \*MAT\_ANISOTROPIC\_ELASTIC\_PLASTIC. This approach can be extended to an anisotropic elasto-plasticity model with rate dependent hardening. For this purpose, the user has to provide the appropriate Lankford-coefficients and hardening curves, while the mapper provides the dominant fiber orientation pointwise. Damage and failure can be added through \*MAT\_ADD\_EROSION.*

*Within the presentation applications of both approaches will be discussed and compared.*

## Introduction to SFRP processing

In automotive industries, the usage of short fiber reinforced plastic (SFRP) components is getting more and more popular, due to the need to build lighter vehicles with the target to reduce CO<sub>2</sub> emissions. Compared to standard materials such as steel or aluminum which phenomenologically can be described as isotropic, these plastic materials show a high degree of anisotropy throughout the whole component and therefore cannot be modeled with standard isotropic elasto-plastic material models such as \*MAT\_024. Through the injection molding process a local varying microstructure with strong anisotropic behavior is induced. It is important for reliable structural simulations to take this local anisotropic material behavior precisely into account.

To be able to do so, the manufacturing history of the component has to be known, namely the processing of the component. Nowadays, quite a few tools exist which allow to predict the fiber

orientation and therefore the degree of anisotropy within such components. The two most common ones being used in industries are Moldflow<sup>®</sup> and Moldex3D<sup>®</sup>. These software tools allow considering applied temperatures and pressures such as they are used within the real manufacturing process as well as the size of the output valve of the tooling and cooling channels. Besides the fiber orientation tensor or its main axis, thermal coefficients and elastic constants can be an output of such simulations, as well as initial stresses.

Fig. 1 shows the schematics of such an injection molding process. Pure glass fiber rovings are cut and mixed with resin material. This is usually a thermoplastic or thermosetting material. Under high pressure and with different temperatures, the molten resin/fiber mixture is injected into the tooling to reach its final geometry.

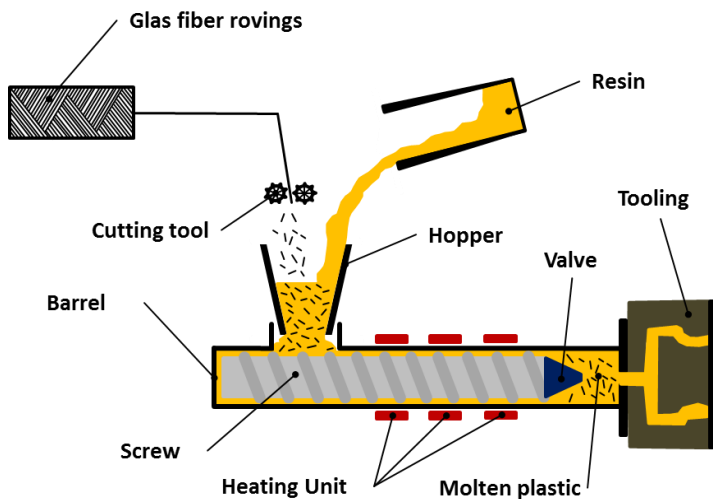


Figure 1: Schematics of the injection molding process for SFRP.

The high degree of anisotropy is caused by the fibers being oriented perpendicular to each other within an inner (core) and an outer (skin) layer. The main axis of the averaged orientation tensors within the outer layer are oriented in the direction of flow whereas the main axis of the orientation tensors of the thinner core layer are oriented perpendicular to the direction of flow. Nevertheless, this varies throughout the whole component and therefore, the processing simulation has to be taken into account to consider the varying stiffness and strength locally.

Fig. 2 shows results from a computer tomographic (CT) scan which can be used to investigate the fiber orientations at certain positions of a component but also to validate the process simulation results. On the left, the averaged values for tensor's main axis components are given over the relative thickness. It can be seen that the orientation in x-direction drops at the center of the component whereas the orientation in y-direction reaches its maximum at this position. Orientations in thickness direction are usually very low. On the right, the values for  $a_{xx}$  are visualized with the \*Initial\_Stress\_Solid - card in LS-PrePost<sup>®</sup>. As mentioned, a clear distinction between skin- and core layer can be made by the color blue indicating a low orientation in x-direction whereas red indicates a high degree of orientation in x-direction.

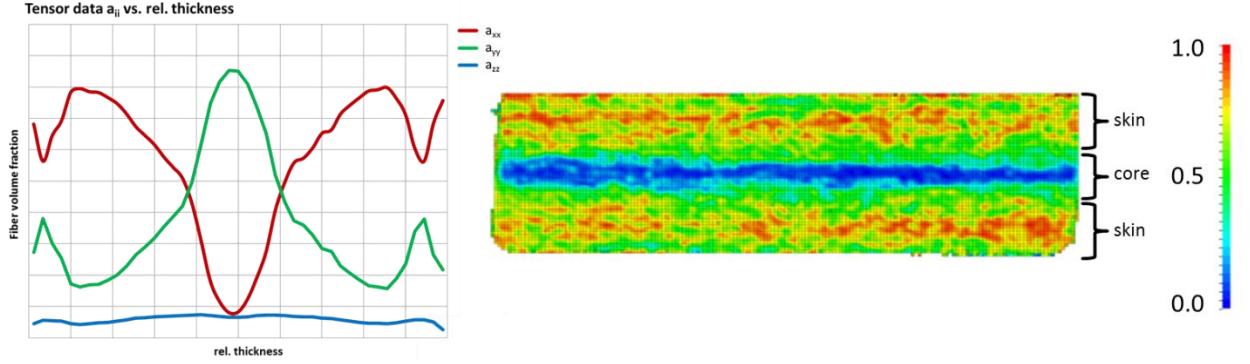


Figure 2: The averaged values for the orientation tensor components of the main axis are shown on the left. On the right, the values for  $a_{xx}$  obtained from CT scans are visualized in LS-PrePost®.

### SFRP process simulation and validation

One of the most important outputs of SFRP process simulations is the fiber orientation tensor, which is a 3x3 symmetric tensor, so usually six values for  $a_{ij} = \{a_{11}, a_{22}, a_{33}, a_{12}, a_{13}, a_{23}\}$  are written to the result files. Commonly, two simulation methods are available to govern the orientation tensor, the Folgar-Tucker equation and the so called Reduced Strain Closure (RSC) method (see Wang et. al. [2008]). The governing equation for the Folgar-Tucker analysis is given by:

$$\frac{Da_{ij}}{Dt} = -\frac{1}{2}(\omega_{ik}a_{kj} - a_{ik}\omega_{kj}) + \frac{1}{2}\lambda(\dot{\gamma}_{ik}a_{kj} + a_{ik}\dot{\gamma}_{kj} - 2a_{ijkl}\dot{\gamma}_{kl}) + 2C_i\dot{\gamma}(\delta_{ij} - 3a_{ij}) \quad (1)$$

with  $a_{ij}$  being the fiber orientation tensor,  $\frac{1}{2}\omega_{ij}$  the vorticity tensor,  $\frac{1}{2}\dot{\gamma}_{ij}$  being the deformation rate tensor, and  $C_i$  being the fiber interaction coefficient which is a phenomenological parameter being determined by fitting to experimental results which are usually obtained from CT scans.

The vorticity tensor is given as:

$$\begin{aligned} \frac{D\boldsymbol{\omega}}{Dt} &= \frac{\partial\boldsymbol{\omega}}{\partial t} + (\mathbf{u} * \nabla) \\ &= (\boldsymbol{\omega} * \nabla)\mathbf{u} - \boldsymbol{\omega}(\nabla * \mathbf{u}) + \frac{1}{\rho^2}\nabla\rho \times p + \nabla \times \left(\frac{\nabla * \boldsymbol{\tau}}{\rho}\right) + \nabla\mathbf{B} \end{aligned} \quad (2)$$

with  $\mathbf{u}$  being the velocity of the flow,  $\rho$  the density,  $p$  the local pressure,  $\boldsymbol{\tau}$  the viscous stress tensor, and  $\mathbf{B}$  the vector for external body forces. For incompressible isotropic fluids this can be reduced to:

$$\frac{\partial\boldsymbol{\omega}}{\partial t} = (\boldsymbol{\omega} * \nabla)\mathbf{v} + \mathbf{v}\nabla^2 * \boldsymbol{\omega} \quad (3)$$

Simulations can be performed with 2D (mid-plane) or 3D meshes. For mid-plane meshes, an additional parameter  $D_z$  is introduced. This parameter is also determined in comparison to experimental results:

$$\frac{Da_{ij}}{Dt} = -\frac{1}{2}(\omega_{ik}a_{kj} - a_{ik}\omega_{kj}) + \frac{1}{2}\lambda(\dot{\gamma}_{ik}a_{kj} + a_{ik}\dot{\gamma}_{kj} - 2a_{ijkl}\dot{\gamma}_{kl}) + 2C_i\dot{\gamma}(\delta_{ij} - (2 + D_z)a_{ij}) \quad (4)$$

Decreasing  $D_z$  leads to a decrease of the out-of-plane orientation and an increase of the thickness of the core layer.

The RSC-method is based on the Folgar-Tucker equation as well. The main idea is to reduce the growth rates of the eigenvalues of the orientation tensor by a scalar value, which is user-defined. The rotation axis of the eigenvalues will be left unchanged:

$$\frac{Da_{ij}}{Dt} = -\frac{1}{2}(\omega_{ik}a_{kj} - a_{ik}\omega_{kj}) + \frac{1}{2}\lambda(\dot{\gamma}_{ik}a_{kj} + a_{ik}\dot{\gamma}_{kj} - 2[a_{ijkl} + (1 - \kappa)(L_{ijkl} - M_{ijmn}a_{mnkl}]\dot{\gamma}_{kl}) + 2\kappa C_i\dot{\gamma}(\delta_{ij} - 3a_{ij}) \quad (5)$$

Thereby,  $\kappa$  is a phenomenological scalar factor and  $[a_{ijkl} + (1 - \kappa)(L_{ijkl} - M_{ijmn}a_{mnkl})]$  is the so called ‘‘closure term’’ with

$$L_{ijkl} = \sum_{p=1}^3 \sigma_p q_i^p q_j^p q_k^p q_l^p$$

$$M_{ijkl} = \sum_{p=1}^3 \sigma_p q_i^p q_j^p q_k^p q_l^p$$

where  $\sigma_p$  is the p-th eigenvalue of  $a_{ij}$  and  $q_i^p$  the i-th component of the p-th eigenvector of the orientation tensor. The RSC method is supposed to give better results compared to the Folgar-Tucker (FT) method when considering a mapping and homogenization of the fiber orientation tensor data for a structural analysis.

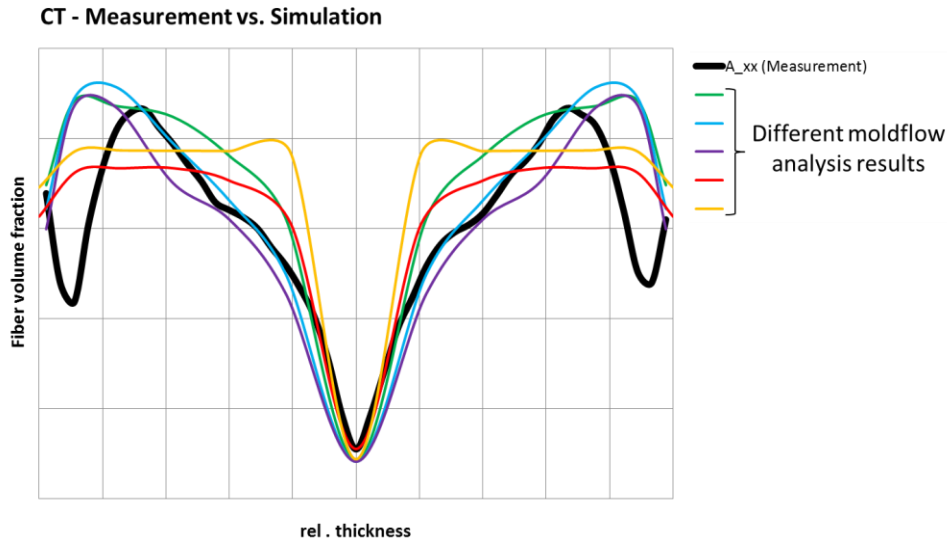


Figure 3: Comparison between simulation results and CT-scan analysis for different parameters for  $C_i$  and  $D_z$  (Folgar-Tucker) and  $C_i$  and  $\kappa$  (RSC).

In fig. 3, a comparison between different values used for both, the RSC and the Folgar-Tucker method and CT scan data is given. The Folgar-Tucker approaches seem to better cover the peaks of the  $a_{xx}$  curve which represents a higher orientation in x-direction at the skin layers whereas the RSC results show an average of these peaks.

The orientation tensor can also be illustrated as an ellipsoid, such as it is shown in fig. 4. The eigenvectors  $\mathbf{q}_i$  of this tensor are the main directions of the fiber distribution, and the eigenvalues  $a_i$  denote the probabilities of fibers lying in the direction of the eigenvectors. For shell discretizations, only the first eigenvector  $\mathbf{q}_1$  is needed, as the second eigenvector lies in the shell plane and is orthogonal to  $\mathbf{q}_1$ . Furthermore, the specification of the first two eigenvalues  $a_1$  and  $a_2$  is sufficient, as  $\sum a_i = 1$ .

fiber-orientation tensor 2<sup>nd</sup> order  $\mathbf{a}$ :

- eigenvectors  $\mathbf{q}_i$  (main fiber directions)
- eigenvalues  $a_i$  (orientation probability)

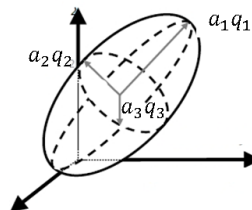


Figure 4: Illustration of the 2<sup>nd</sup> order orientation tensor  $\mathbf{a}$ .

## Data transfer and homogenization

### Mapping:

In order to perform a proper data mapping, one has to know which data shall be transferred between the different meshes and in which format these data are written to the standard output file formats which for Moldflow<sup>®</sup> or Moldex3D<sup>®</sup> are usually either an ascii or xml file. The data is given as either the values of the full fiber orientation tensor as it was introduced above  $\{a_{11}, a_{22}, a_{33}, a_{12}, a_{13}, a_{23}\}$ , or as its eigenvalues and the corresponding eigenvectors. It is quite common that the unit system for the process simulation (e.g. kg-m-s) is different from the unit system being used for the structural analysis (e.g. kg-mm-ms). This has to be considered, as well as the case that the meshes are defined within different coordinate systems. Therefore, a data

mapping program should be able to perform a geometry matching as well. Additionally, the number of integration points being used for the process simulation is usually different from the number of integration points being used in the structural analysis. A standard Moldflow<sup>®</sup> simulation for example considers 13 integration points through the thickness whereas a crash application usually runs with up to five integration points in order to save calculation time. Furthermore, the element type and size might be different, so a proper homogenization and averaging has to be performed. This problem is illustrated in fig. 5.

These requirements are being fulfilled within the data mapper being developed at the DYNAmore GmbH, called DYNAmap. By now, a standard closest point search is realized and no homogenization or data averaging is performed. In order to save calculation time, a bucket sort algorithm is implemented. A geometry matching is realized by allowing the user to define several nodal IDs within the source and target mesh which shall be matched. The data mapper cannot only be used for the transfer of SFRP process simulation data, but also to perform data mapping between process simulations being done in LS-DYNA (e.g. metal forming) where stresses, thicknesses and history variables (e.g. GISSMO damage parameters) can be transferred. Within one of the next releases, an averaging and homogenization of scalar and tensorial values shall be realized according to the work of Gahm [2014] and Shepard [1968]. Main challenge for the tensorial averaging is to obtain the shape (eigenvalues and eigenvectors) and the orientation of the tensorial data. For the averaging of scalar values, a direction dependency and distance weighting shall be considered.

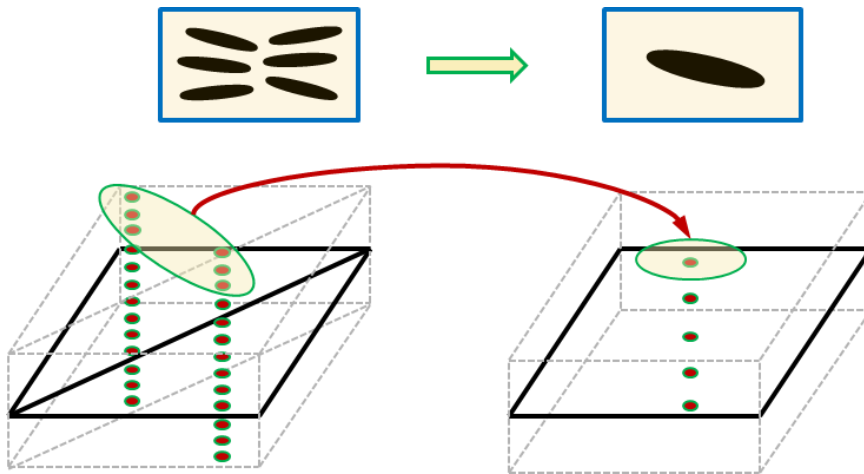


Figure 5: Mapping of tensorial data between different meshes and mesh sizes with varying number of through-thickness integration points.

#### Analytical elastic homogenization:

Mlekusch [1997] described an analytical homogenization procedure for evaluating the 21 anisotropic composite stiffness values in two steps, as shown in fig. 6.

In a first step, homogenized stiffness values for a pseudo-composite with aligned fibers embedded in an infinite matrix material are computed, as there are analytical solutions and estimations available in the literature for this case. This can for example be the procedure of Mori & Tanaka [1973]. For this, the 4<sup>th</sup> order Eshelby-Tensor  $\mathbf{E}$ , that depends on the geometry and lateral straining properties of the inclusion has to be evaluated, see Mura [1987] and the so called strain concentration tensor (4<sup>th</sup> order)

$$\mathbf{A}^{Eshelby} = \left( \mathbf{I} + \mathbf{E} : \mathbf{S}^m : (\mathbf{C}^f - \mathbf{C}^m) \right)^{-1} \quad (6)$$

for a dilute fiber concentration can be evaluated.  $\mathbf{C}^f$ ,  $\mathbf{C}^m$  and  $\mathbf{S}^m$  stand for the fiber and matrix stiffness tensor, and the matrix compliance. For realistic fiber concentrations the strain concentration tensor

$$\mathbf{A}^{MT} = \mathbf{A}^{Eshelby} : ((\mathbf{1} - \nu_f)\mathbf{I} + \nu_f \mathbf{A}^{Eshelby})^{-1} \quad (7)$$

should be used for more accurate results.  $\nu_f$  denotes the fiber volume fraction and  $\mathbf{I}$  stands for the unit tensor 4<sup>th</sup> order. The homogenized elastic stiffness tensor for this unidirectional “pseudo-composite” can then be calculated as

$$\mathbf{C}^{UD} = \mathbf{C}^m + \nu_f (\mathbf{C}^f - \mathbf{C}^m) : \mathbf{A}^{MT}. \quad (8)$$

In a second step, the actual fiber distribution at the integration point is taken into account. This could be performed in a very descriptive way as a spatial integration of the unidirectional stiffness tensor multiplied with the orientation distribution function  $\psi$ . The homogenized stiffness tensor could then be evaluated as

$$\mathbf{C} = \int \mathbf{C}^{UD}(\theta, \phi) \psi(\theta, \phi) d\Omega. \quad (9)$$

Advani & Tucker [1987] transformed this spatial integral into a tensorial formulation based on the fiber orientation tensors 2<sup>nd</sup> and 4<sup>th</sup> order  $\mathbf{a}_2$  and  $\mathbf{a}_4$ , which is more convenient for numerical evaluation. The homogenized stiffness tensor is then given by

$$\begin{aligned} C_{ijkl} = & B_1 a_{ijkl} + B_2 (a_{ij} \delta_{kl} + a_{kl} \delta_{ij}) + B_3 (a_{ik} \delta_{jl} + a_{il} \delta_{jk} + a_{jl} \delta_{ik} + a_{jk} \delta_{il}) + B_4 (\delta_{ij} \delta_{kl}) \\ & + B_5 (\delta_{ik} \delta_{jl} + \delta_{il} \delta_{jk}) \end{aligned} \quad (10)$$

The factors  $B_1 - B_5$  contain the components of the unidirectional stiffness tensor  $\mathbf{C}^{UD}$ , as given in fig. 6. While the 2<sup>nd</sup> order fiber orientation tensor  $\mathbf{a}_{ij}$  is usually known, the 4<sup>th</sup> order fiber orientation tensor  $\mathbf{a}_{ijkl}$  has to be estimated by a so called closure approximation, see for example Dray et al. [2007].

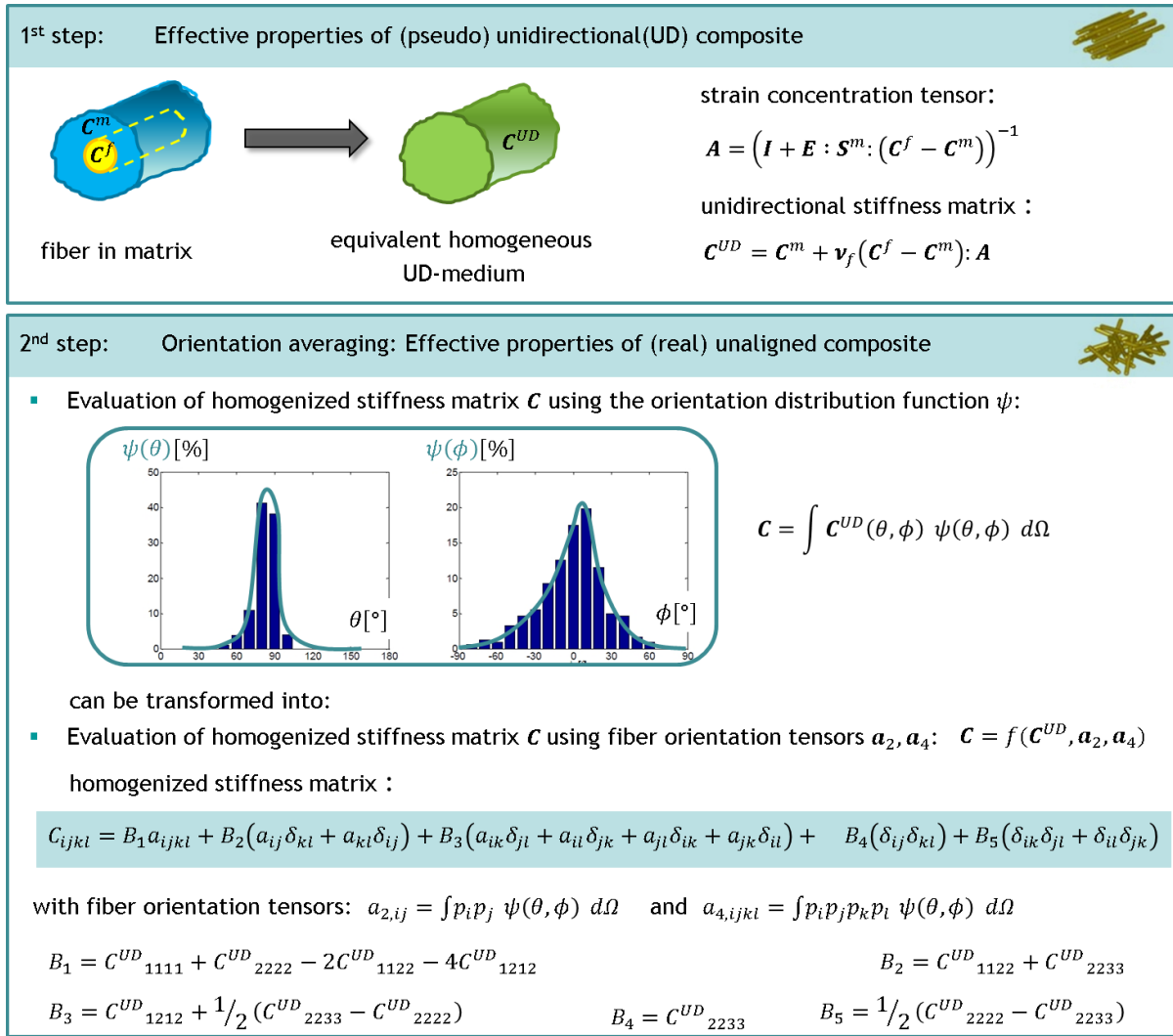


Figure 6: Analytical elastic homogenization.

**Inelastic analytical homogenization:**

The approach of analytical homogenization for elastic material behavior can be extended for inelastic material behavior (see Reithofer et al. [2012], Kaiser & Stommel [2012]), as shown in fig. 7. In order to avoid the evaluation of the composites homogenized inelastic stiffness tensor (material tangent) for each strain state, the fiber orientation averaging is performed with the strain concentration tensor  $\mathbf{A}$ , applying the strategy of Advani & Tucker [1987]. Using this orientation averaged strain concentration tensor  $\bar{\mathbf{A}}$ , for each strain increment  $\Delta \boldsymbol{\varepsilon}^c$  of the composite, the strain increment proportion concerning the matrix material

$$\Delta \bar{\boldsymbol{\varepsilon}}^M = (\nu_F \bar{\mathbf{A}} + (1 - \nu_F) \mathbf{1})^{-1} : \Delta \bar{\boldsymbol{\varepsilon}}^c \quad (11)$$

and the fiber strain increment

$$\Delta \bar{\boldsymbol{\varepsilon}}^F = \frac{1}{\nu_F} (\Delta \bar{\boldsymbol{\varepsilon}}^c - (1 - \nu_F) \Delta \bar{\boldsymbol{\varepsilon}}^M) \quad (12)$$

are evaluated. For the fibers, elastic behavior is assumed until failure and the corresponding fiber stress increment is given by



$$\Delta\bar{\sigma}^F = \mathbf{C}^{el,f} : \Delta\bar{\epsilon}^F \tag{13}$$

The matrix material is assumed to behave isotropic elasto-visco-plastic using a von Mises plasticity formulation. The current matrix stress increment is evaluated by a return mapping algorithm. And the desired current homogenized composite stress increment

$$\Delta\bar{\sigma}^c = v_F \Delta\bar{\sigma}^F + (1 - v_F) \Delta\bar{\sigma}^M \tag{14}$$

can hence be evaluated. From time to time, the strain concentration tensor  $\mathbf{A}$  and its orientation averaging  $\bar{\mathbf{A}}$  is updated.

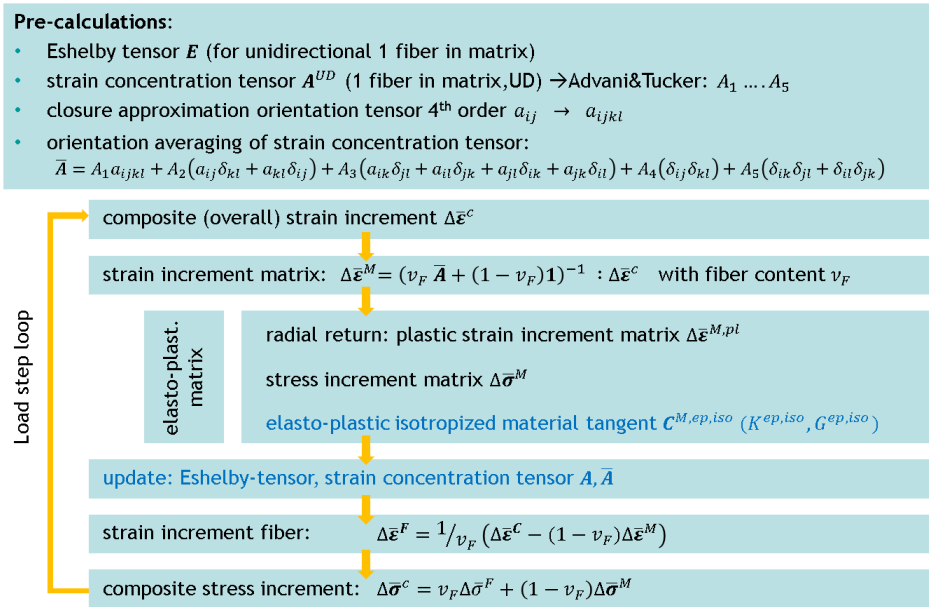


Figure 7: Analytical inelastic homogenization, realized in \*MAT\_4a\_Micromec (\*MAT\_215).

### Modeling approaches for structural analysis

While for UD or fabric reinforced composites standard macroscopic anisotropic material models can be applied, for injection molded composites, we have to deal with local varying anisotropy. Thus we need constitutive models that can capture and handle this local anisotropic behavior. The fiber-matrix – interaction taking place on the micro-scale shall be integrated on the macroscopic scale through homogenization for each integration point.

To this end, the information about the local fiber orientation tensor is needed, and has to be transferred from a molding simulation to the structural model by an appropriate data mapper.

Furthermore, homogenization strategies are needed. For this purpose two options will be available in LS-DYNA, as shown in fig. 8. One possibility is to evaluate homogenized elastic material properties and homogenized material parameters for anisotropic inelastic material models, for example Hill-Plasticity, for each integration point by an appropriate data mapper (e.g. DYNAmap) and transfer this information as history variables for \*MAT\_ANISOTROPIC\_ELASTIC\_PLASTIC (\*MAT\_157). The second possibility is to use the mapper solely for transferring the fiber orientation tensor to the structural simulation model,

while the homogenization is performed within the material model \*MAT\_4a\_MICROMECH (\*MAT\_215), developed by 4a Engineering®.

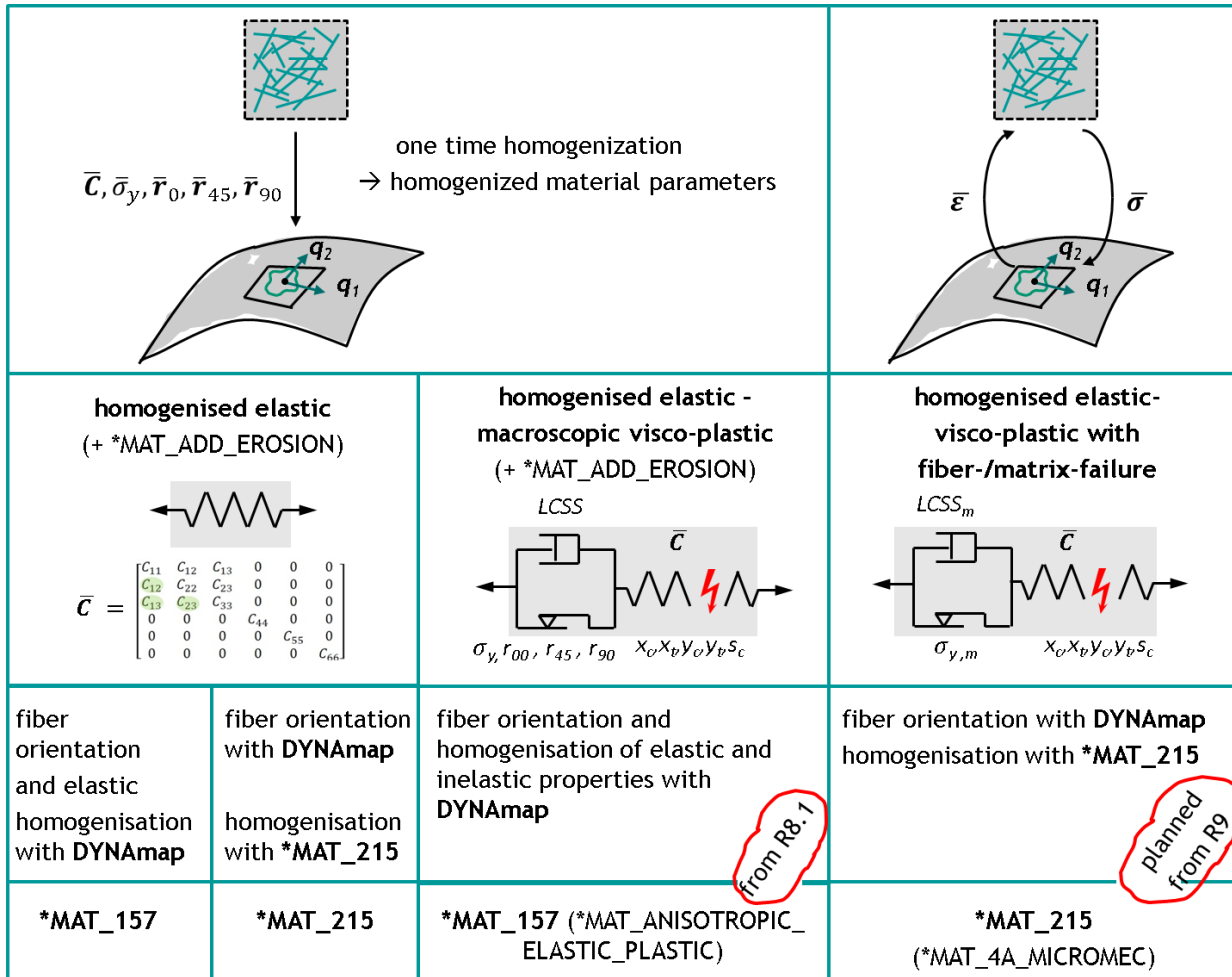


Figure 8: Integrative simulation: possibilities with LS-DYNA

For both cases, the data mapper writes the necessary information as history variables for the material model in the keywords \*INITIAL\_STRESS\_SOLID or \*INITIAL\_STRESS\_SHELL respectively. Thus one material keyword card can be used for a structural part, despite the varying material behavior in each integration point, see fig. 9. Comparable simulation approaches were already introduced by Nutini & Vitali [2010] and Hatt [2014]. Both introduce a failure modeling using \*MAT\_ADD\_EROSION with the GISSMO option with a strain based failure in matrix direction and a stress based failure in fiber direction. This will be applied as well for the application given below. An alternative would be the usage of the newly implemented Tsai-Wu failure criterion in \*MAT\_157 which allows defining failure strengths in fiber and matrix direction in tension and compression.

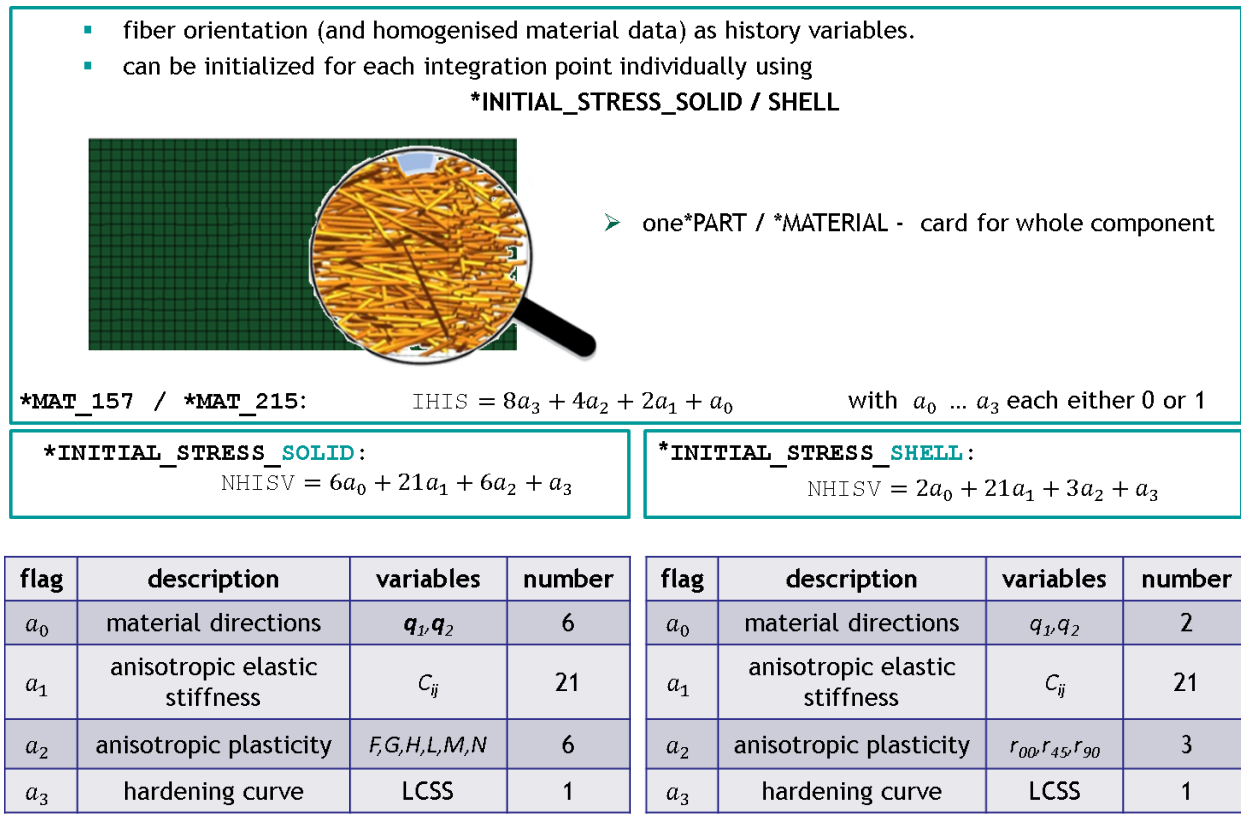


Figure 9: Initialization of local varying material properties through `*INITIAL_STRESS_OPTION`.

**A) Simulation with `*MAT_ANISOTROPIC_ELASTIC_PLASTIC (*MAT_157)`:**

The usage of `*MAT_157` allows the user to define a local stiffness  $C_{ij}$ , its orientation  $q_1$  and  $q_2$  as well as to define values for the anisotropic plasticity ( $r_{00}, r_{45}, r_{90}$ ) and locally varying hardening curves. The initialization is applied using the `IHIS` – flag in the material card as well as the respective value for `NHISV` in the `*INITIAL_STRESS_OPTION` – card (see fig. 9). These values can be defined for each integration point and derived using `DYNAMap`. The stiffness values can be defined directly using the respective orientation data from process analysis in combination with the stiffness properties of the fiber and the matrix material as well as geometrical parameters. The elastic homogenization will be performed by `DYNAMap` as it is described above.

In order to derive the plasticity curves, experimental data should be at hand for at least a  $0^\circ$  and a  $90^\circ$  specimen, a  $45^\circ$  specimen might improve the results of the interpolation between the plasticity curves which can be fitted using optimization approaches within `LS-OPT`<sup>®</sup>. Experiments should also be performed at different velocities in order to consider a strain rate dependency of the matrix material. A table definition instead of a hardening curve in the `*INITIAL_STRESS_OPTION` – allows to account for this strain rate dependency in the material model. For the numerical example given below, the plasticity curves were derived as follows:

1. The orientation is assumed to be constant through the thickness, and the  $0^\circ$  plasticity curve is derived by fitting simulation data to the  $0^\circ$  experiments.
2. Orientation is assumed to be perpendicular through the thickness (skin-core-effect). Therefore, the plasticity curve for the middle integration point is assumed to be the one of

the 0° experiments, and the 90° plasticity curve is derived by fitting the simulation to the 90° experiments.

3. Evaluation is performed on the 0° simulation/experiments, now considering perpendicular orientations through the thickness.
4. Plasticity curves for 45° can be derived independently, assuming that the behavior in 45° is equal to an orientation in 135°.
5. Curve interpolation is performed by DYNAmap in steps of 5°, in order to derive curves for all orientations between 0° and 90°.

It has to be considered, that for a proper data interpolation, the plasticity curves may not intersect each other. Therefore, a rather simple approach would be to scale the derived 0° plasticity curve in order to fit the experimental data. Fig. 10 gives an overview on recommended experiments and the curve interpolation.

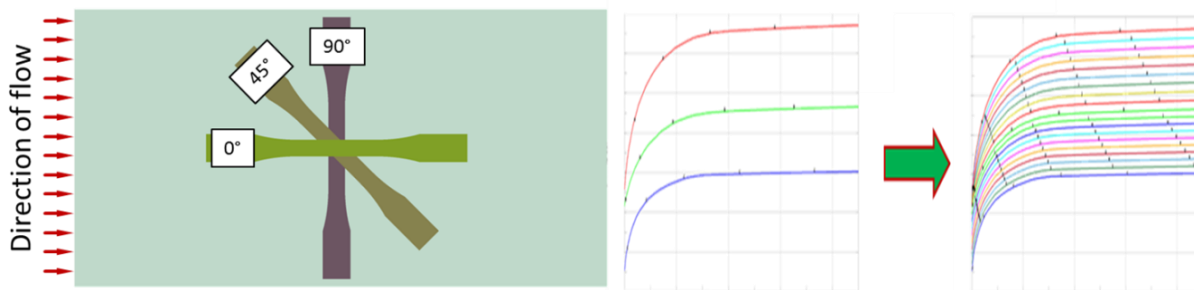


**Figure 10: Experiments performed for material parameter identification for \*MAT\_157 and interpolation of plasticity curves.**

A very similar approach is chosen to fit failure parameters for the \*MAT\_ADD\_EROSION – card using the GISSMO damage and failure model. In a first step, strength parameters are fitted to consider failure in 0° direction. In a second step, strain parameters are fitted to consider failure in matrix direction. Evaluation is then performed for the 45° specimen.

#### **B) Simulation with \*MAT\_4a\_MICROMECH (\*MAT\_215):**

The integration of the recently by 4a Engineering® developed \*MAT\_4a\_MICROMECH in LS-DYNA is planned from revision R9.0 for solids and shells. It allows for analytical homogenization for elastic and as well for inelastic elastic material behavior of fiber or particle reinforced materials, as described above in fig. 6 and fig. 7.

The user only needs to provide the information of the elastic properties of the fiber material as well as fiber failure values and the elasto-viscoplastic matrix material, and geometrical information about the fiber reinforcement, as cylinder, elliptical cylinder, circle (for example for voids), plate, the aspect ratio  $asp=r1/r2$  of the reinforcement and the fiber volume fraction. The user can choose between a purely elastic simulation, or an elasto-viscoplastic simulation and between different closure approximation approaches. In addition the fiber orientation tensor, in terms of the main values and main directions has to be provided, either as history variable through \*INITIAL\_STRESS\_OPTION, or for example for an application with UD-composites directly in the material card through defining the material direction via AOPT and related data together with the main values a11 and a22 of the fiber orientation tensor.

## Numerical example

With the proposed modeling approach, it is possible to fit simulation data to experiments in 0°, 45°, and 90° direction. The procedure introduced above was used for this task. It has to be considered that \*MAT\_157 only offers an elastic-viscoplastic material description, whereas in the experiments, a high degree of visco-elasticity can be observed, especially for the highest strain rate. The results are shown in fig. 11. The results for the failure modeling are also acceptable.

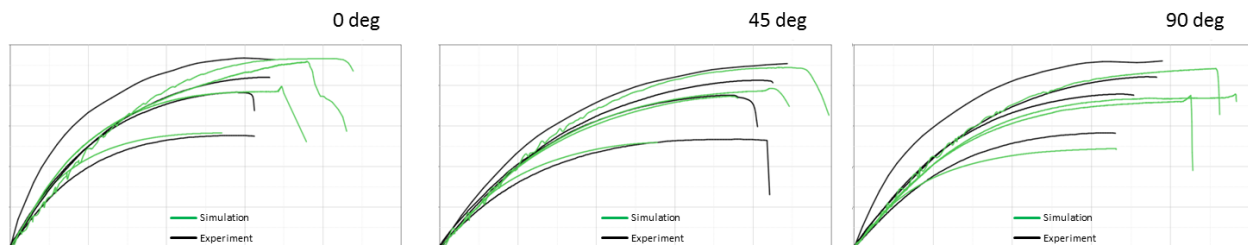


Figure 11: Simulation vs. experiment for \*MAT\_157 parameter fitting.

## Conclusion and outlook

It was shown, how data from injection molding simulations can be used within LS-DYNA with recent enhancements on \*MAT\_157. In order to properly transform the process simulation results, the data mapper being developed at DYNAmore, DYNAmap was being introduced. A modeling strategy was being developed and presented, showing the necessity to fully consider the process simulation within the structural analysis. Furthermore, a newly developed material model was introduced, \*MAT\_4a\_MICROMECH (\*MAT\_215), which shall consider the full micromechanics of the material.

The next steps include the application of \*MAT\_215 for the presented experiments as well as the testing of the newly implemented Tsai-Wu criteria within \*MAT\_157. Further improvements on the mapping procedure will include a tensor averaging and homogenization.

## References

- |                         |   |
|-------------------------|---|
| Dvorak [2013]           | Dvorak, G., Micromechanics of Composite Materials, Springer Heidelberg, 2013.   |
| Advani & Tucker [1987]  | Advani, S. G., Tucker, C. L., Journal of Rheology, The Use of Tensors to Describe and Predict Fiber Orientation in Short Fiber Composites, 31 (8), (1987), 751-784.   |
| Dray et al. [2007]      | Dray, D., Gilormini, P., Regnier, G., Comparison of several closure approximations for evaluating the thermoelastic properties of an injection molded short fiber composite. Composites Science and Technology, Elsevier, (2007), pp.1601-1610. |
| Kaiser & Stommel [2012] | Kaiser, j.-M., Stommel, M., An Extended Mean-Field Homogenization Model to Predict the Strength of Short-Fibre Polymer Composites, TECHNISCHE MECHANIK, 32, 2-5, (2012), 307 - 320  |
| Mlekusch [1997]         | Mlekusch, B., Kurzfaserverstärkte Thermoplaste, Dissertation, Montanuniversität Leoben (1997)   |
| Mori & Tanaka [1973]    | Mori T, Tanaka K., Average stress in matrix and average elastic energy of materials with misfitting inclusions. Acta Metall (1973), 21:571-574.   |
| Mura [1987]             | Mura, T.: Micromechanics of Defects in Solids, Kluwer Academic Publishers, 1987.  |
| Reithofer et al. [2012] | Reithofer, P., Jilka, B., Fertschaj, A., 4a micromec für die integrative Simulation faserverstärkter Kunststoffe. 10 <sup>th</sup> LS-DYNA-Forum, Ulm (2012).   |

- Wang et. al. [2008] J. Wang, J.F. O’Gara, and C.L. Tucker III, An Objective Model for Slow Orientation Dynamics in Concentrated Fiber Suspensions: Theory and Rheological Evidence. *Journal of Rheology*, 52(5):1179-1200 (2008).
- Shepard [1968] Shepard, D., A two-dimensional interpolation function for irregularly-spaced data, Proceeding ACM National Conference, 1968.
- Gahm [2014] Gahm, J. K., Microstructural Feature-based Processing and Analysis of Diffusion Tensor MRI, PhD Thesis, University of California, USA, 2014.
- Nutini & Vitali [2010] Nutini, M., Vitali, M., Simulating anisotropy with LS-DYNA in glass-reinforced, polypropylene-based components. 9<sup>th</sup> LS-DYNA Forum, Bamberg (2010).
- Hatt [2014] Hatt, A., Anisotropic modeling of short fibers reinforced thermoplastics materials with LS-DYNA. 13<sup>th</sup> LS-DYNA Forum, Bamberg (2014).